Hindawi
Advances in Civil Engineering
Volume 2022, Article ID 6069871, 11 pages
https://doi.org/10.1155/2022/6069871

Research Article

Machine Learning-Based Model in Predicting the Plate-End Debonding of FRP-Strengthened RC Beams in Flexure

Tianyu Hu and Guibing Li

School of Management Science and Engineering, Shandong Technology and Business University, Yantai, Shandong 264005, China

Correspondence should be addressed to Tianyu Hu; 1459430123@qq.com

Received 22 November 2021; Revised 8 February 2022; Accepted 2 March 2022; Published 24 March 2022

Academic Editor: AFAQ AHMAD

Reinforced concrete (RC) beams strengthened with fiber reinforced polymers (FRPs) are structurally complex and prone to plate-end (PE) debonding. In this study, considering the extremely complicated nonlinear relationship between the PE debonding and the parameters, machine learning algorithms, namely, linear regression, ridge regression, decision tree, random forest, and neural network improved by sparrow search algorithm, are established to predict the PE debonding of RC beams strengthened with FRP. The results of reliability evaluation and parameter analysis reveal that ACI, CNR, fib-1, fib-2, and TR55-2 are a little conservative; AS and TR55-1 have the problem of overestimating the shear force; the accuracy and robustness of the SSA-BP model developed in this paper are good; the stirrup reinforcement has the greatest effect on PE debonding; and each parameter shows a complex nonlinear relationship with the shear force when PE debonding occurs.

1. Introduction

The lightweight, high strength, and high corrosion resistance of fiber reinforced polymers (FRPs) make it widely used in the repair and rehabilitation of existing concrete structures [1]. Nevertheless, a large number of experimental studies have demonstrated that external FRP improves the load carrying capacity of RC beams, but due to the linear elasticity characteristics of the material itself, debonding failure often occurs after strengthening, which greatly limits its use in practical applications [2–8]. There are two main types of debonding failure in FRP-strengthened RC beams in flexure: plate-end (PE) debonding and intermediate crack (IC) debonding. For beams with small shear span, since the bending moment is minor at this time, the beam is mainly subjected to shear force and PE debonding is very likely to occur. Concrete cover separation and plate-end interfacial debonding are the two modes of PE debonding. Generally, plate-end interfacial debonding occurs merely when the width of the FRP sheet is much smaller than the width of the strengthened beam. Therefore, concrete cover separation is the more common mode of PE debonding. When the terminal of FRP is close to the support, the concrete cover separation is mainly caused by the shear crack at the end of FRP. As the load increases, the shear cracks develop to cause vertical and horizontal displacement in the concrete beam and thus generate interfacial shear stress and normal stresses. With the increase in stress, the concrete cover will separate when the crack reaches the horizontal plane of the tensile reinforcement [9, 10]. When the terminal of FRP is far away from the support, the inclined cracks are generated in the shear area, and when the inclined cracks reach the level of the tensile reinforcement, the cracks spread in the horizontal direction and lead to the splitting of the concrete cover [11, 12]. In order to solve the problem of limiting the use of FRP due to PE debonding, end anchoring is usually used to prevent it. And, in order to better design the end-anchoring system, it is necessary to first determine the shear force when PE debonding occurs.

Researchers and codes have developed different computational models for PE debonding of FRP-strengthened RC beam based on the shear force of the concrete beam and the debonding strain of FRP. Most of these models are based on shear strength of the beams or based on fracture mechanics. Oehlers developed a strength model based on the shear force and bending moment acting at the plate end in 1992 [9]. Jansze proposed a plate-end debonding strength model, which was originally developed for steel-plated beams in 1997. The proposed model considered the occurrence of PE debonding failure at the onset of shear cracking in RC beams [13]. Ahmed and van Germert modified the model of Jansze considering the differences between FRP and steel properties and the effect of shear reinforcement in 1999 [14]. Smith and Teng proposed a model that is based on the concrete shear strength only in 2002 [15]. A theoretical model based on truss analogy was proposed by Colotti and others in 2004 to predict the failure mode and ultimate capacity of FRP-strengthened RC beams [16]. Yao and Teng and Teng and Yao conducted experimental and analytical investigations on FRP-strengthened beams in 2007, thus modifying the moment shear interaction expression proposed by Oehlers [17, 18]. The fib Bulletin 14 (fib, 2001) presented the model proposed by Blaschko which is based on the concrete shear strength of the beam. The Technical Report 55 (TR55) of the Concrete Society (2012), ACI 440.2 R (ACI, 2017), and Australian Standard AS 5100.8 (Standards Australia, 2017b) recommended an upper limit for the acting shear force at the plate-end region to avoid PE debonding. El-sayed and others proposed a model which is based on the concrete shear strength of the beams considering main parameters known to affect the opening of the shear cracks and consequently affect PE debonding in 2021 [19]. Nevertheless, due to the complex structure of FRP-strengthened RC beams and the nonlinear relationship between PE debonding and parameters, most of the above models suffer from low computational accuracy and poor robustness. Therefore, it is especially important to establish a more precise nonlinear mapping relationship between PE debonding and each parameter.

Given the large number of parameters that affect the PE debonding, this study uses several machine learning algorithms, namely, linear regression, ridge regression, decision tree, random forest, and neural network optimized by the sparrow search algorithm to develop several intelligent prediction models for PE debonding of FRP-strengthened RC beams and then select the best prediction model from it. Based on the best model obtained, the robustness of the model and the codes are assessed and the parameters affecting PE debonding are analyzed too.

2. Parameter Identification and Data Collection

2.1. Parameter Identification. Based on relevant codes and experimental studies [13–24], concrete strength (f′c), location of FRP cut-off point (Lua/*a*), tensile strength of tensile reinforcement (fy), tensile strength of stirrup reinforcement (fyv), stirrup reinforcement ratio (*ρ*sv), tensile strength of FRP (ffu), FRP stiffness (Eftf), and the ratio of FRP width to the width of the strengthened beam (bf/b) are selected as input parameters for predicting PE debonding in this study. For the convenience of establishing the model, the above parameters are denoted as X1, X2, X3 X4, X5, X6, X7, and X8, respectively, and the shear force is taken as the output of models and denoted as V.

2.2. Criteria for Collection Analysis of Parameters

(1) PE debonding occurred in all strengthened beams [6–8, 17, 25–52].

(2) The FRP sheets are not prestressed and the end of the strengthened beams is not anchoraged.

(3) The geometric and material properties of the strengthened beams, FRP, and reinforcement are clear.

(4) The range of parameter variation is large and basically covers the case of general beams. The range of the variation of each parameter is shown in Figure 1.

From Figure 1, we can get that the maximum interval of f′c is 30 MPa–40 MPa, accounting for 49%, and merely 6% of the f′c is more than 60 MPa, indicating that the f′c is mostly at plain level; the maximum interval of the Lua/*a* is 0.8–1.0, accounting for 64%, while other intervals account for less; the design value of fyv is mainly distributed from 250 MPa to 510 MPa, accounting for 69%, and only 6% of the strength is over 570 MPa, indicating that the fyv is mostly at ordinary level, and high-strength reinforcement accounts for a relatively small percentage; the maximum interval of *ρ*sv is 0.6–0.9, accounting for 38%, and the distribution of each range is more uniform; the maximum interval of ffu is 3000 MPa–4000 MPa, accounting for 54%, and the tensile strength above 4000 MPa accounts for only 9%; the maximum interval of the fy is 350 MPa–510 MPa, accounting for 51%, but the percentage of tensile strength over 510 MPa is 49%, indicating that a larger portion of tensile reinforcement in the collected specimens is high-strength reinforcement; the maximum interval of Eftf is from 75 MPa to 125 MPa, accounting for 40%, and only 8% above 225 MPa; the maximum interval of the bf/b is > 0.9, accounting for 37%, and the distribution of each interval is relatively uniform. In addition, some of the parameters differed significantly across intervals, which would result in machine learning models having smaller prediction errors in intervals with more data than in intervals with less data.

3. Machine Learning Models

This part uses several machine learning algorithms, namely, linear regression, ridge regression, decision tree, random forest, and neural network optimized by sparrow search algorithm to develop several intelligent prediction models for PE debonding of FRP-strengthened RC beams. The data are used from [6–8, 17, 25–52], where the percentages of training set, validation set, and testing set are 60%, 20%, and 20%, respectively.

To further analyze the prediction accuracy and generalization ability of each model, the average absolute error (MAE) and goodness-of-fit (R2) of the training set, the validation set, and the testing set of the models are calculated and given in Figure 2.

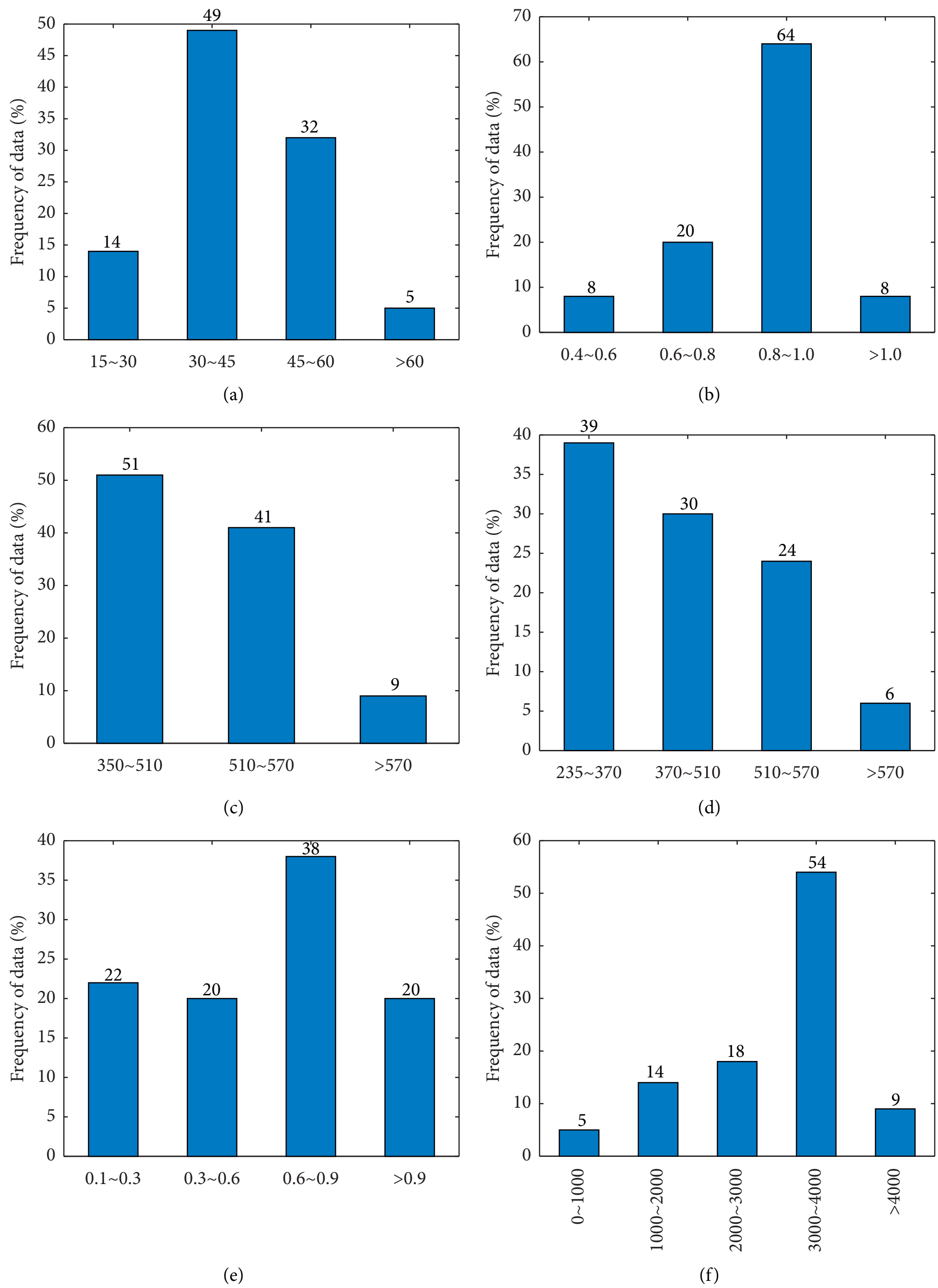

Figure 1: Continued.

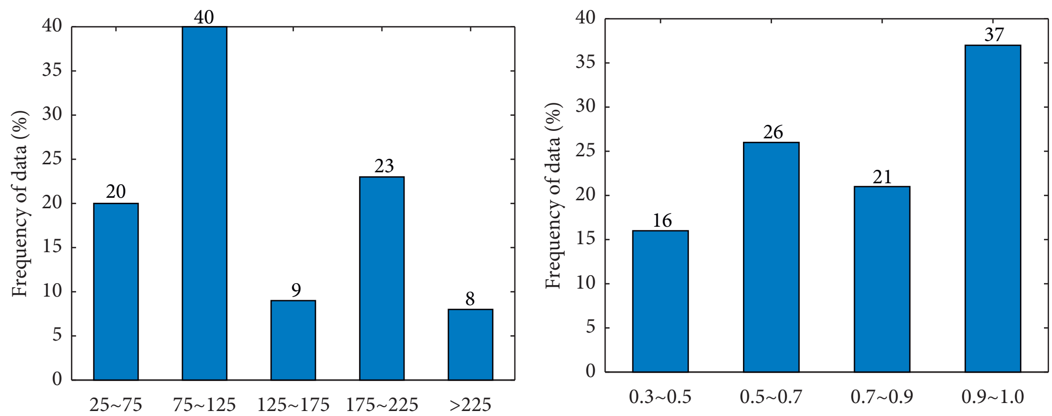

(g) (h)

Figure 1: Range of the parameters. (a) f'c/MPa. (b) Lua/a. (c) fy/MPa. (d) fyv/MPa. (e) ρsv. (f) ffu/MPa. (g) Eftf/GPa.mm. (h) bf/b.

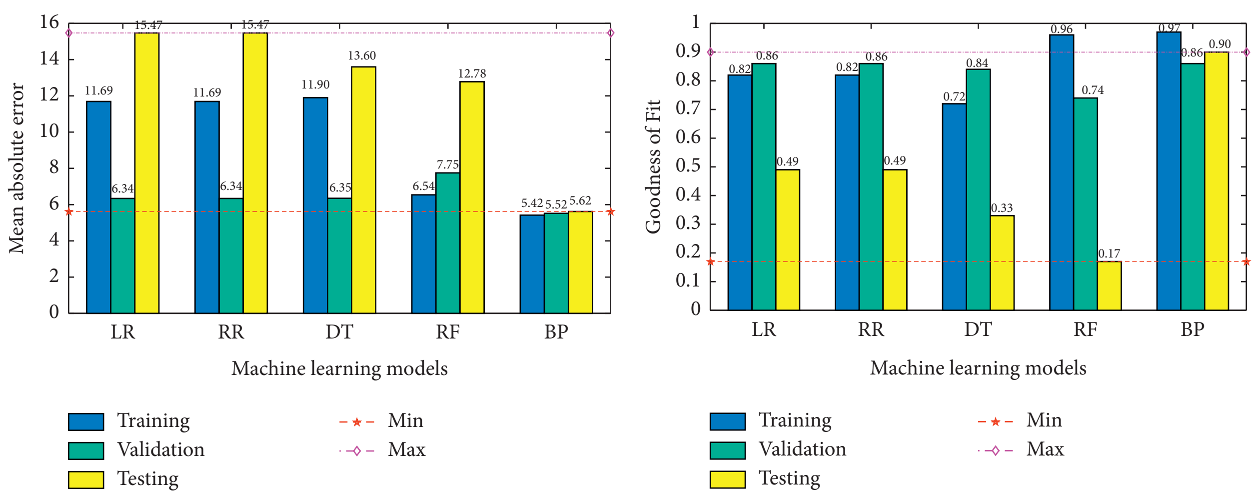

(a) (b)

Figure 2: Performance of the models. (a) MAE. (b) R2.

From Figure 2, the MAE and the R2 of linear regression, ridge regression, decision tree, and random forest differ greatly in the training set, the validation set, and the testing set, indicating that the generalization ability of these models is poor, while the MAE of BP neural network is 5.42, 5.52, and 5.62 in the training set, the validation set, and the testing set, respectively, which is not only the smallest but also the most average among all machine learning algorithms. Also, the R2 of the training set, the validation set, and the testing set of the BP neural network is 0.97, 0.86, and 0.90, respectively, which is the highest among all machine learning models. In summary, the BP neural network model not only has the highest prediction accuracy but also has excellent generalization ability.

4. Reliability Evaluation of the Code

To further illustrate the precision and robustness of the SSA-BP, this section compares it with several international codes [13–17]. The codes and their expressions are shown in Table 1, and the comparison between the calculated and actual values of SSA-BP and the codes is shown in Figure 3.

It can be visualized from Figure 3 that the calculated values of SSA-BP are basically within 15% above and below the true value and are significantly superior to the calculated values given by each code. The calculated values of ACI and fib-1 are basically below 15% of the true value, indicating that these two codes are too conservative; while AS and TR55-1 have a larger portion of calculated values above 15% of the true value, which takes the risk of overestimating the shear strength in the event of PE debonding. The quantitative evaluation of the performance of BP and each code is shown in Table 2.

As can be seen from Table.2, the coefficient of variation of the neural network is merely 20.3%, which is better than the calculated values of each code. The coefficients of variation of CNR and fib-1 and TR55-2 are smaller, but their conservative estimates account for 79%, 80%, and 95%,

Table 1: Codes and their expressions.

Codes	Calculation formula
ACI440.2 R	$V_{db,\text{end}} < 0.67V_c$
AS 5100.8	$V_{db,\text{end}} < 0.67V_u$
Fib-1	$V_{\text{db,end}} < 0.15 f_{ck}^{1/3}\text{bd}$
Fib-2	$\varepsilon_{f\,d} = \begin{cases} \alpha_1 c_1 k_c k_b \sqrt{f_{ct}/n_{frp}E_{frp}t_{frp}} & l_b \geq l_{b,\max} \\ \alpha_1 c_1 k_c k_b \sqrt{f_{ct}/n_{frp}E_{frp}t_{f\,rp}} \cdot (l_b/l_{b,\max})(2 - l_b/l_{b,\max}) & l_b < l_{b,\max} \end{cases}$ $l_{b,\max} = \sqrt{(n_{frp}E_{frp}t_{frp})/(c_2 f_{ct})}$ $k_b = 1.06\sqrt{(2b_{frp}/b)/(1 + b_{frp}/400)} \geq 1$ $b_{frp}/b \geq 0.33$
TR55-1	$V_{db,\text{end}} < 0.67V_{rd}$
TR55-2	$\varepsilon_{f\,d} = \begin{cases} 0.5k_b\sqrt{f_{ct}/n_{frp}E_{frp}t_{frp}} & l_b \geq l_{b,\max} \\ 0.5k_b\sqrt{f_{ct}/n_{frp}E_{frp}t_{f\,rp}} \cdot (l_b/l_{b,\max})(2 - l_b/l_{b,\max}) & l_b < l_{b,\max} \end{cases}$ $l_{b,\max} = 0.7\sqrt{n_{frp}E_{frp}t_{frp}/f_{ct}}$
CNR	$\varepsilon_{f\,d} = \begin{cases} 1/\gamma_{f,d}\sqrt{2\Gamma_{F\,d}/n_{frp}E_{frp}t_{frp}} & l_b \geq l_{b,\max} \\ 1/\gamma_{f,d}\sqrt{2\Gamma_{F\,d}/n_{frp}E_{frp}t_{frp}} \cdot (l_b/l_{b,\max}) & l_b < l_{b,\max} \end{cases}$ $\Gamma_{F\,d} = k_b k_G\sqrt{f_c' f_{ct}}$ $k_b = \begin{cases} \sqrt{(2 - b_{frp}/b)/(1 + b_{frp}/b)} \geq 1 & b_{frp}/b \geq 0.25 \\ 1.18 & b_{frp}/b < 0.25 \end{cases}$ $l_{b,\max} = \min\left\{(1/\gamma_{R\,d}f_{b\,d})\sqrt{\pi^2 E_{frp}t_{frp}\Gamma_{F\,d}/2}, 200\text{mm}\right\}$ $f_{b\,d} = 2\Gamma_{F\,d}/S_u$

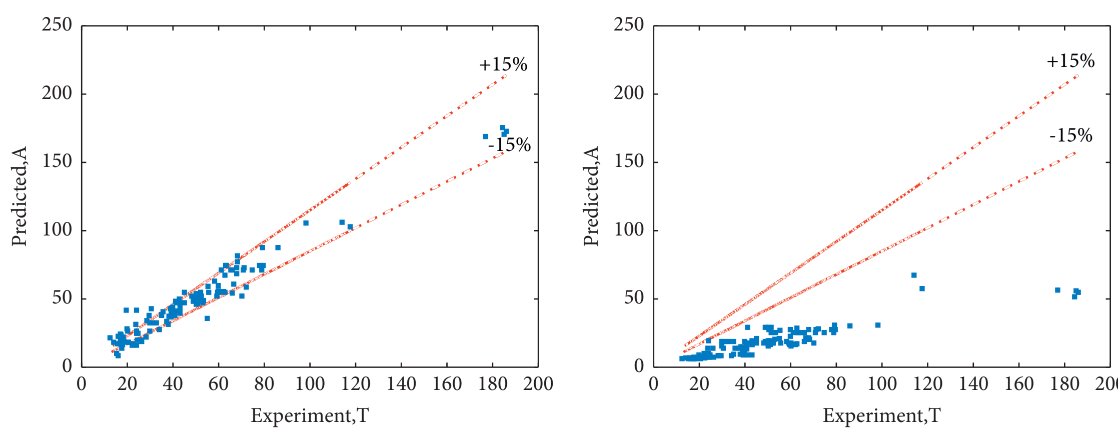

(a) (b)

Figure 3: Continued.

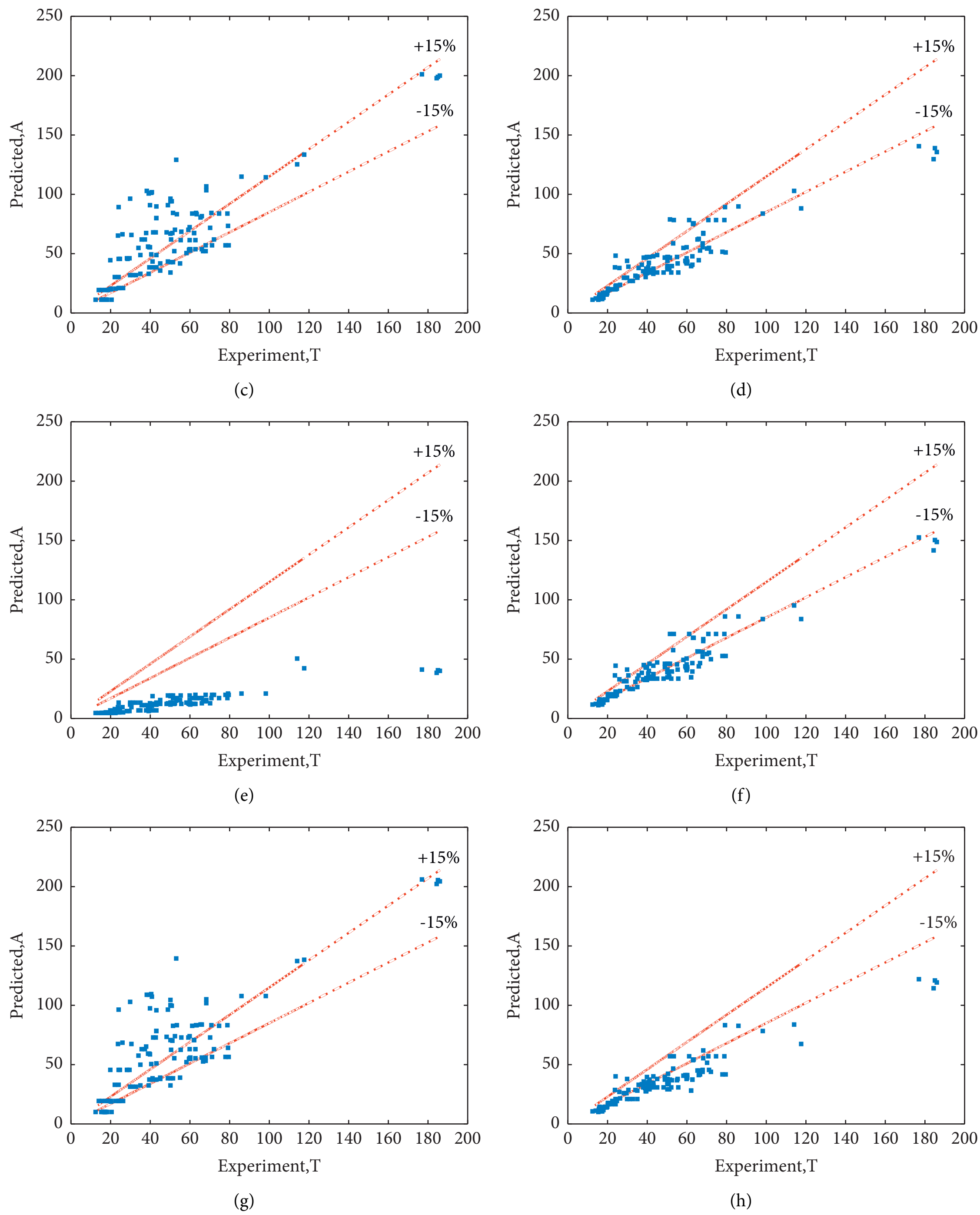

FIGURE 3: Comparison of the calculated values and real values. (a) SSA-BP. (b) ACI. (c) AS. (d) CNR. (e) fib-1. (f) fib-2. (g) TR55-1. (h) TR55-2.

TABLE 2: Performance of the models.

Models	Evaluation indicators		
	Coefficient of variation (%)	Conservative (%)	Nonconservative (%)
SSA-BP	20.3	52	48
ACI	26.6	100	0
AS	44.5	38	63
CNR	23.4	79	21
Fib-1	25.1	100	0
Fib-2	21.2	80	20
TR55-1	48.3	39	61
TR55-2	20.5	95	5

Table 3: Weights and biases between connection layers.

	Hidden layer							Output
	H(1 : 1)	H(1 : 2)	H(1 : 3)	H(1 : 4)	H(1 : 5)	H(1 : 6)	H(1 : 7)	V
Bias	.743	.529	2.692	.061	−1.476	.038	.776	
X1	.022	1.514	.906	.179	.279	.443	−.473	
X2	−.095	−.656	−.243	.438	.662	−.188	−1.296	
X3	−.348	.946	−.998	−.395	.900	−.240	.362	
X4	−.037	.765	−.727	.350	−.142	−.096	−1.060	
X5	−.006	.782	1.731	.816	−.139	.281	−.277	
X6	−.681	−.587	−.845	−.428	−.135	−.695	.584	
X7	.272	1.773	−.444	.053	.583	−.030	1.619	
X8	1.225	.077	−.300	.169	.669	.940	.993	
Bias								1.115
H(1 : 1)								−1.425
H(1 : 2)								.381
H(1 : 3)								−2.224
H(1 : 4)								.511
H(1 : 5)								−1.377
H(1 : 6)								1.147
H(1 : 7)								.736

respectively, which are a little conservative compared with 50% for SSA-BP.

5. Parametric Study

5.1. Analysis of the Importance of Parameters. In Matlab software, by inputting the 'net.iw', the'net.lw', and the 'net.b', the weights and biases of the neural network can be obtained. See Table 3 for details.

After getting the weights and biases between layers, we can get the transfer functions through the code 'TransferFcn' in Matlab. The transfer functions are shown in equation (1) and (2).

$$y_i = f \cdot \left(\sum_i w_{ij} x_i + \phi_j \right) = \frac{2}{1 + e^{-2\left(\sum_i w_{ij} x_i + \phi_j\right)}} - 1. \quad (1)$$

$$y_i = f \cdot \left(\sum_i w_{ij} x_i + \phi_j \right) = \sum_i w_{ij} x_i + \phi_j. \quad (2)$$

The weights and biases obtained in Table 1 were substituted into (1) and (2) and subsequently normalize the calculated value obtained to get the importance of each parameter on PE debonding, as shown in Figure 4.

As can be seen from Figure 4, the importance of each parameter is *X*5>X7>*X*2>X1>*X*8>X4>*X*3>X6 in order; that is, the ρsv has the greatest effect on the PE debonding, and the ffu, fy, and fyv have less effect on it.

5.2. Sensitivity Analysis of Parameters. Based on the effects of each parameter on PE debonding obtained in section 5.1, the ffu, which has the least effect on PE debonding, is selected as the grouping variable for the sensitivity analysis of each parameter, and four grades of 200, 1200, 2200, and 3200 are taken based on its distribution in section 2.1. When studying the sensitivity of a single variable to PE debonding, the other variables are averaged based on the statistics in section 1.2.

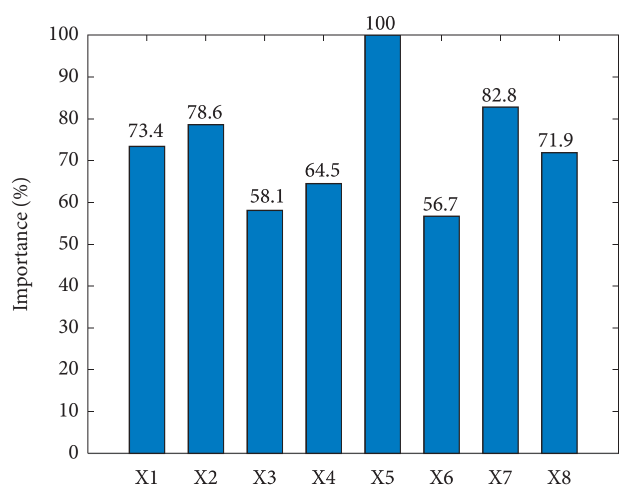

Figure 4: Importance of each parameter.

The sensitivity of each parameter to the shear strength is shown in Figure 5.

From Figure 5, we can get that (a) when the ffu is in the first two grades, the shear strength tends to increase and subsequently decrease with the increase in f'c. When it is in the last two grades, the shear strength tends to increase, subsequently decrease, and then increase as the f'c increases; (b) for the Lua/*a*, the shear strength increases and subsequently decreases with the increase in the Lua/*a*, regardless of the grade of ffu; (c) regarding the ρsv, no matter which grade the ffu is at, as the ρsv increases, the shear strength first decreases, then increases, and then decreases; (d) for the fyv, there are three patterns when the ffu is in different grades, namely, when the ffu is in two grades of 200 and 1200, the shear strength is inversely proportional to the increase in fyv; when the ffu is in grade 2200, the shear strength tends to decrease and subsequently increase with the increase in fyv; when the ffu is in grade 3200, the shear strength is proportional to the fyv; (e) for Eftf and bf/b, as they increase, the

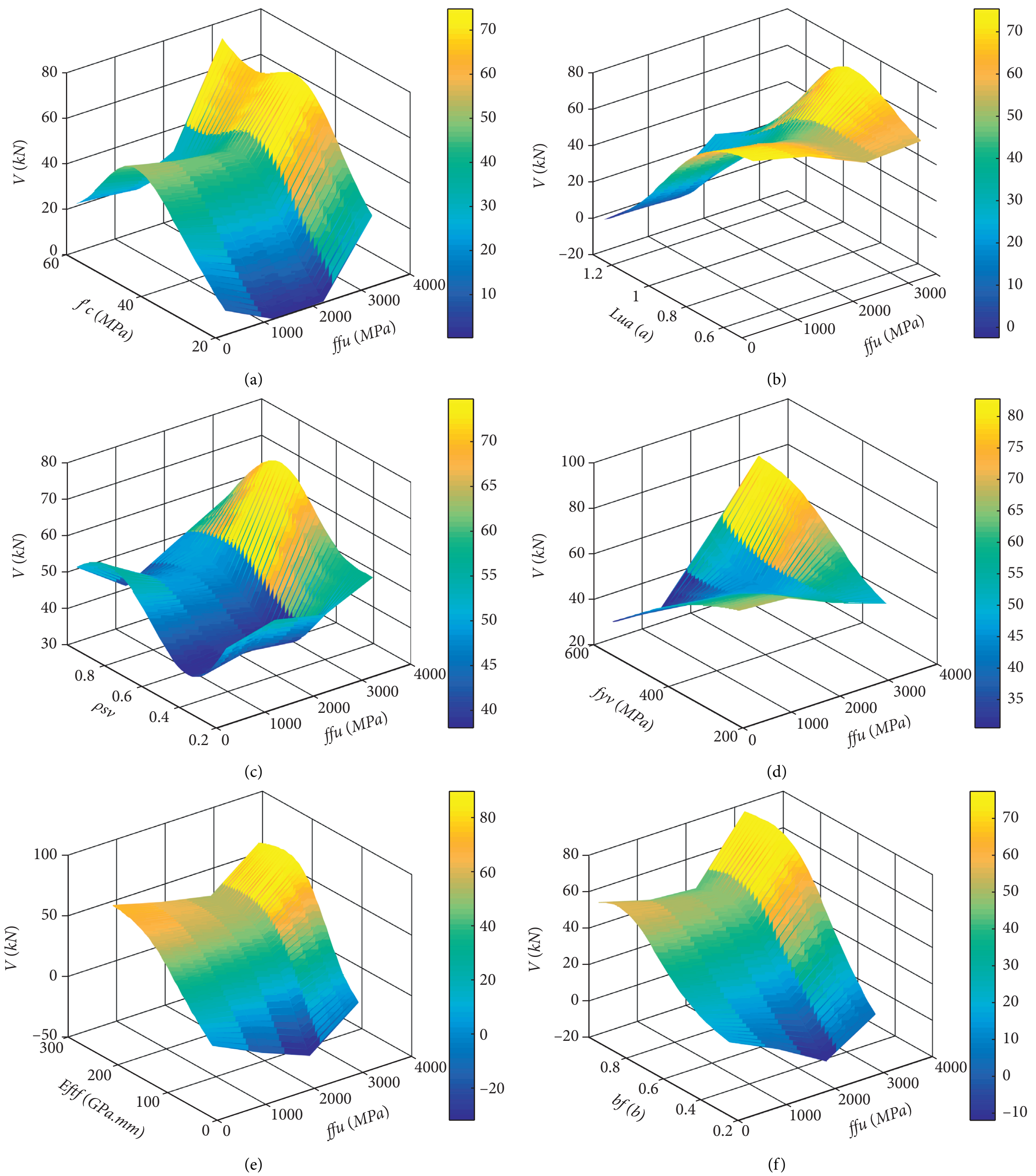

Figure 5: Sensitivity of each parameter.

shear strength basically increases and subsequently decreases, but when the Eftf and bf/b are larger, the shear strength decreases not significantly.

In summary, there is a complex nonlinear relationship between the shear force at PE debonding and each parameter. In the future, the effect of different parameters on PE debonding under different conditions needs to be considered when performing the end anchorage system.

6. Conclusion

In this study, a machine learning approach was used to synthesize the effects of various parameters on the PE debonding of FRP-strengthened RC beams in flexure, and the resulting models were evaluated against several codes. The following conclusions can be drawn:

(1) ACI, CNR, fib-1, fib-2, and TR55-2 are too conservative, which have 100%, 80%, 100%, 79%, and 95% values below the experimental values, respectively. AS and TR55-1 had 63% and 61% values above the experimental values, respectively, potentially overestimating the shear force in the case of PE debonding. The coefficient of variation, conservative, and nonconservative values of SSA-BP is 20.3%, 52%, and 48%, respectively, and its robustness and prediction accuracy are superior to the above codes.

(2) ρsv, Eftf, and Lua/a have more influence on the shear force at PE debonding, while fy and ffu have less influence on the shear force. Moreover, there are complex nonlinear relationships between each parameters and the shear force, and the effect of different parameters on PE debonding under different conditions needs to be considered when performing the system of end anchorage in the future.

(3) There are two problems with the model built in this paper: on the one hand, the uneven distribution of parameters in the dataset on which the model is built leads to the prediction accuracy of the model to be improved, and on the other hand, the model is complicated by considering too many parameters. In the future, more data need to be collected and the parameters in the model need to be streamlined.

Notation

f'c: Compressive strength of concrete
ρsv: Stirrup reinforcement ratio
fy: Tensile strength of tensile reinforcement
fyv: Tensile strength of stirrup reinforcement
Eftf: FRP stiffness
bf/b: The ratio of sheet width to beam width
Lua/a: The ratio of anchorage length to shear span
ffu: Tensile strength of FRP
fct: Tensile strength of concrete
Vdb, end: Factored shear force at the FRP plate end
Vc: The shear capacity of concrete alone calculated according to ACI 318 (ACI Committee 318, 2014)
Vu: The nominal shear strength of the concrete section including concrete and steel stirrups, calculated in accordance with AS 5100.5 (2017)
fck: The characteristic strength of concrete calculated according to BS EN 1992-1-1 (2004)
Vrd: The shear strength of the beam section calculated in accordance with Section 6.2.3 of BS EN 1992–1-1 (2004)
lb, max: The maximum anchorage length
Γfd: The design value of the specific fracture energy of the FRP-concrete interface.

Data Availability

The data for the study were collected from articles by different researchers and have been marked in the article.

Conflicts of Interest

The authors declare that there are no conflicts of interest.

References

[1] R. Kotynia, E. Oller, A. Marí, and M. Kaszubska, "Efficiency of shear strengthening of RC beams with externally bonded FRP materials - state-of-the-art in the experimental tests," *Composite Structures*, vol. 267, Article ID 113891, 2021.

[2] R. Bakay, E. Y. Sayed-Ahmed, and N. G. Shrive, "Interfacial debonding failure for reinforced concrete beams strengthened with carbon-fibre-reinforced polymer strips," *Canadian Journal of Civil Engineering*, vol. 36, no. 1, pp. 103–121, 2009.

[3] F. Ceroni, M. Pecce, S. Matthys, and L. Taerwe, "Debonding strength and anchorage devices for reinforced concrete elements strengthened with FRP sheets," *Composites Part B: Engineering*, vol. 39, no. 3, pp. 429–441, 2008.

[4] J. Pan, C. K. Y. Leung, and M. Luo, "Effect of multiple secondary cracks on FRP debonding from the substrate of reinforced concrete beams," *Construction and Building Materials*, vol. 24, no. 12, pp. 2507–2516, 2010.

[5] M. A. Al-Saawani, A. K. El-Sayed, and A. I. Al-Negheimish, "Assessment of plate-end debonding design provisions for RC beams strengthened with FRP," *Latin American Journal of Solids and Structures*, vol. 17, 2020.

[6] M. A. Al-Saawani, A. K. El-Sayed, and A. I. Al-Negheimish, "Effect of basic design parameters on IC debonding of CFRP-strengthened shallow RC beams," *Journal of Reinforced Plastics and Composites*, vol. 34, no. 18, pp. 1526–1539, 2015.

[7] P. J. Fanning and O. Kelly, "Ultimate response of RC beams strengthened with CFRP plates," *Journal of Composites for Construction*, vol. 5, no. 2, pp. 122–127, 2001.

[8] D. M. Nguyen, T. K. Chan, and H. K. Cheong, "Brittle failure and bond development length of CFRP-concrete beams," *Journal of Composites for Construction*, vol. 5, no. 1, pp. 12–17, 2001.

[9] D. J. Oehlers, "Reinforced concrete beams with plates glued to their soffits," *Journal of Structural Engineering*, vol. 118, no. 8, pp. 2023–2038, 1992.

[10] S. S. Zhang and J. G. Teng, "End cover separation in RC beams strengthened in flexure with bonded FRP reinforcement: simplified finite element approach," *Materials and Structures*, vol. 49, no. 6, pp. 2223–2236, 2016.

[11] M. Achintha and C. J. Burgoyne, "Fracture mechanics of plate debonding: validation against experiment," *Construction and Building Materials*, vol. 25, no. 6, pp. 2961–2971, 2011.

[12] P. M. M. Achintha and C. J. Burgoyne, "Fracture mechanics of plate debonding," *Journal of Composites for Construction*, vol. 12, no. 4, pp. 396–404, 2008.

[13] W. Jansze, *Strengthening of RC members in bending by externally bonded steel plates*, PhD thesis, Delft University of Technology, South Holland, Netherlands, 1997.

[14] O. Ahmed and D. Van Gemert, "Effect of longitudinal carbon fiber reinforced plastic laminates on shear capacity of reinforced concrete beams," in *Proceedings of the 4th International Symposium on Fiber Reinforced Polymer Reinforcement for Reinforced Concrete Structures*, Maryland, MD, USA, 1999.

[15] S. T. Smith and J. G. Teng, "FRP-strengthened RC beams. II: assessment of debonding strength models," *Engineering Structures*, vol. 24, no. 4, pp. 397–417, 2002.

[16] V. Colotti, G. Spadea, and R. N. Swamy, "Structural model to predict the failure behavior of plated reinforced concrete beams," *Journal of Composites for Construction*, vol. 8, pp. 104–122, 2004.

[17] J. Yao and J. G. Teng, "Plate end debonding in FRP-plated RC beams-I: Experiments," *Engineering Structures*, vol. 29, no. 10, pp. 2457–2471, 2007.

[18] J. G. Teng and J. Yao, "Plate end debonding in FRP-plated RC beams-II: strength model," *Engineering Structures*, vol. 29, no. 10, pp. 2472–2486, 2007.

[19] A. K. El-Sayed, M. A. Al-Saawani, and A. I. Al-Negheimish, "Empirical shear based model for predicting plate end debonding in frp strengthened rc beams," *Journal of Civil Engineering and Management*, vol. 27, no. 2, pp. 117–138, 2021.

[20] International Federation for Structural Concrete (fib), Externally bonded FRP reinforcement for RC structures. Technical Report, Task Group 9.3, Bulletin No. 14, Lausanne, Switzerland, 2001.

[21] Concrete Society, "Design guidance for strengthening concrete structures using fibre composite materials," Technical Report No. 55, Crowthorne, London, UK, 2012.

[22] American Concrete Institute, "Guide for the design and construction of externally bonded FRP systems for strengthening concrete structures," Farmington Hills, Michigan, MI, USA, ACI 440.2R, 2017.

[23] Standards Australia, "Bridge design, Part 8: rehabilitation and strengthening of existing bridges," SA1 Global Limited, Australia, AS 5100.8, 2017.

[24] National Research Council, "Guide for the design and construction of externally bonded FRP systems for strengthening existing structures," CNR-DT 200 R1, Rome, Italy, 2013.

[25] P. A. Ritchie, D. A. Thomas, L. W. Lu, and G. M. Conelly, "External reinforcement of concrete beams using fibre reinforced plastics," *ACI Structural Journal*, vol. 88, no. 4, pp. 490–500, 1991.

[26] R. J. Quantrill, L. C. Hollaway, and A. M. Thorne, "Experimental and analytical investigation of FRP strengthened beam response: Part I," *Magazine of Concrete Research*, vol. 48, no. 177, pp. 331–342, 1996.

[27] M. Arduini, A. Di Tommaso, and A. Nanni, "Brittle failure in FRP plate and sheet bonded beams," *ACI Structural Journal*, vol. 94, no. 4, pp. 363–370, 1997.

[28] H. N. Garden, L. C. Hollaway, and A. M. Thorne, "A preliminary evaluation of carbon fibre reinforced polymer plates for strengthening reinforced concrete members," *Proceedings of the Institution of Civil Engineers - Structures and Buildings*, vol. 122, no. 2, pp. 127–142, 1997.

[29] H. N. Garden, R. J. Quantrill, L. C. Hollaway, A. M. Thorne, and G. A. R. Parke, "An experimental study of the anchorage length of carbon fibre composite plates used to strengthen reinforced concrete beams," *Construction and Building Materials*, vol. 12, no. 4, pp. 203–219, 1998.

[30] A. J. Beber, A. C. Filho, and J. L. Campagnolo, "Flexural strengthening of R/C beams with CFRP sheets," in *Proceedings of the 8th International Conference on Advanced Composites for Concrete Repair*, London, UK, 1999.

[31] E. David, C. Djelal, E. Ragneau, and F. B. Bodin, "Use of FRP to strengthen and repair RC beams: experimental study and numerical simulations," in *Proceedings of the 8th International Conference on Advanced Composites for Concrete Repair*, London, UK, 1999.

[32] K. M. Hau, "Experiments on concrete beams strengthened by bonding fibre reinforced plastic sheets," MSc in Civil Engineering thesis, The Hong Kong Polytechnic University, Hong Kong, China, 1999.

[33] G. Tumialan, P. Serra, A. Nanni, and A. Belarbi, "Concrete cover delamination in reinforced concrete beams strengthened with carbon fiber reinforced polymer sheets," in *Proceedings of the 4th International Symposium on Fiber Reinforced Polymer Reinforcement for Reinforced Concrete Structures*, pp. 725–735, Maryland, MA, USA, 1999.

[34] O. A. F. Ahmed, *Strengthening of R. C. beams by means of externally bonded CFRP laminates: improved model for plateend shear*, PhD Thesis, Department of Civil Engineering, Catholicke University of Leuven, Catholicke, Belgium, 2000.

[35] S. Matthys, *Structural behavior and design of concrete beams strengthened with externally bonded FRP reinforcement*, PhD thesis, Ghent University, Ghent, Belgium, 2000.

[36] B. Gao, W. Leung, C. Cheung, J. K. Kim, and C. K. Y. Leung, "Effects of adhesive properties on strengthening of concrete beams with composite strips," in *Proceedings of the International Conference on FRP composites in Civil Engineering*, pp. 423–432, Elsevier, 2001.

[37] M. Maalej and Y. Bian, "Interfacial shear stress concentration in FRP-strengthened beams," *Composite Structures*, vol. 54, no. 4, pp. 417–426, 2001.

[38] H. Rahimi and A. Hutchinson, "Concrete beams strengthened with externally bonded FRP plates," *Journal of Composites for Construction*, vol. 5, no. 1, pp. 44–56, 2001.

[39] S. T. Smith and J. G. Teng, "Shear-bending interaction in debonding failures of FRP-plated RC beams," *Advances in Structural Engineering*, vol. 6, no. 3, pp. 183–199, 2003.

[40] M. Valcuende, J. Benlloch, and C. J. Parra, "Ductility of reinforced concrete beams strengthened with CFRP strips and fabric," in *Proceedings of the 6th International Symposium on FRP Reinforcement for Concrete Structures*, pp. 337–346, 2003.

[41] S. F. Breña and B. M. Macri, "Effect of carbon-fiber-reinforced polymer laminate configuration on the behavior of strengthened reinforced concrete beams," *Journal of Composites for Construction*, vol. 8, no. 3, pp. 229–240, 2004.

[42] B. Gao, J. K. Kim, and C. K. Y. Leung, "Taper ended FRP strips bonded to RC beams: experiments and FEM analysis," in *Proceedings of the 2nd International Conference on FRP in Civil Engineering*, pp. 399–405, 2004.

[43] B. Gao, J.-K. Kim, and C. K. Y. Leung, "Experimental study on RC beams with FRP strips bonded with rubber modified resins," *Composites Science and Technology*, vol. 64, no. 16, pp. 2557–2564, 2004.

[44] N. F. Grace and S. B. Singh, "Durability evaluation of carbon fiber-reinforced polymer strengthened concrete beams: experimental study and design," *ACI Structural Journal*, vol. 102, no. 1, pp. 40–48, 2005.

[45] H. B. Pham and R. Al-Mahaidi, "Prediction models for debonding failure loads of carbon fiber reinforced polymer retrofitted reinforced concrete beams," *Journal of Composites for Construction*, vol. 10, no. 1, pp. 48–59, 2006.

[46] O. Benjeddou, M. B. Ouezdou, and A. Bedday, "Damaged RC beams repaired by bonding of CFRP laminates," *Construction and Building Materials*, vol. 21, no. 6, pp. 1301–1310, 2007.

[47] M. R. Esfahani, M. R. Kianoush, and A. R. Tajari, "Flexural behaviour of reinforced concrete beams strengthened by CFRP sheets," *Engineering Structures*, vol. 29, no. 10, pp. 2428–2444, 2007.

[48] F. Ceroni, "Experimental performances of RC beams strengthened with FRP materials," *Construction and Building Materials*, vol. 24, no. 9, pp. 1547–1559, 2010.
[49] A. K. Al-Tamimi, R. Hawileh, and J. Abdalla, "Effects of ratio of CFRP plate length to shear span and end anchorage on flexural behavior of SCC RC beams," *Journal of Composites for Construction*, vol. 15, no. 6, pp. 908–919, 2011.
[50] A. Sadrmomtazi, H. Rasmi Atigh, and J. Sobhan, "Experimental and analytical investigation on bond performance of the interfacial debonding in flexural strengthened RC beams with CFRP sheets at tensile face," *Asian Journal of Civil Engineering (BHRC)*, vol. 15, no. 3, pp. 391–410, 2014.
[51] A. Hasnat, M. Islam, and A. Amin, "Enhancing the debonding strain limit for CFRP-strengthened RC beams using U-clamps: identification of design parameters," *Journal of Composites for Construction*, vol. 20, no. 1, Article ID 04015039, 2016.
[52] T. Skuturna and J. Valivonis, "Experimental study on the effect of anchorage systems on RC beams strengthened using FRP," *Composites Part B: Engineering*, vol. 91, pp. 283–290, 2016.